



PERGAMON

Available online at www.sciencedirect.com

SCIENCE @ DIRECT®

Scripta Materialia 49 (2003) 411–415



www.actamat-journals.com

Strain gradients and geometrically necessary dislocations in deformed ice single crystals

Maurine Montagnat ^{a,*}, Paul Duval ^a, Pierre Bastie ^b, Bernard Hamelin ^c

^a *Laboratoire de Glaciologie et Géophysique de l'Environnement, CNRS, BP 96, 38402 St Martin d'Hères Cedex, France*

^b *Laboratoire de Spectrométrie Physique, CNRS, BP 87, 38402 St Martin d'Hères Cedex, France*

^c *Institut Laue Langevin, BP 156X, 38042 Grenoble Cedex 9, France*

Received 11 April 2003; received in revised form 20 May 2003; accepted 22 May 2003

Abstract

Hard X-ray diffraction experiments were performed on ice single crystals deformed in torsion. This work shows the relationship between the density of geometrically necessary dislocations and strain gradients. The torsion strain appears to be totally accommodated by geometrically necessary basal screw dislocations.

© 2003 Acta Materialia Inc. Published by Elsevier Science Ltd. All rights reserved.

Keywords: Strain-gradient plasticity; Ice; X-ray diffraction; Dislocation structure

1. Introduction

There has recently been great interest in developing mechanism-based theories of strain-gradient plasticity including an internal length scale, to describe the deformation of crystalline materials on the micron scale [1–4]. Strain gradients can be caused by the loading geometry. Strengthening effects arising from strain gradients are observed in indentation and torsion experiments on the micron scale [1,3]. In torsion, strength increases with decreasing wire diameter. These results are interpreted in terms of geometrically necessary dislocations associated with strain gradients. Strain

gradients can also be induced in polycrystals by the mismatch of slip at boundaries [1,5]. Large spread of orientations was found in grains of aluminium alloys after deformation in plane strain compression by using the back scattering diffraction technique (EBSD) [6,7]. The concept of geometrically necessary dislocations was used as the central tool in the description of such deformation inhomogeneities [8].

Geometrically necessary dislocations play a key role in the modelling of size-dependent plasticity. The hardening associated with these dislocations becomes significant when plastic deformation takes place on small scales [9–11]. The relevant size scale to consider in strain-gradient plasticity theory is the scale associated with the dislocation structure that evolves during deformation. There is hence a great need for experimental characterisation of geometrically necessary dislocations associated with non-uniform plastic deformation [12,13].

* Corresponding author. Tel.: +33-4-76-82-42-18; fax: +33-4-76-82-42-01.

E-mail address: maurine@lgge.ujf-grenoble.fr (M. Montagnat).

The density of geometrically necessary dislocations has already been estimated for a few ice samples from polar ice sheets [14]. In ice polycrystals, strain gradients can be induced by the mismatch of slip at the boundaries, greatly enhanced by the strong plastic anisotropy of ice crystals. Ice essentially deforms by the activity of the basal slip systems $\langle 11\bar{2}0 \rangle (0001)$ [15]. With such behaviour, the length scale at which strain gradients significantly influence flow-stress increments is expected to be very large in ice.

The purpose of this work is to estimate the nature and density of geometrically necessary dislocations associated with strain gradients resulting from torsion tests on ice single crystals on a scale of several millimeters. Hard X-ray diffraction experiments were carried out to characterise the geometrically necessary dislocations required to accommodate the lattice distortion and to evaluate their density. Emphasis is placed on the relationship between geometrically necessary dislocations and hardening.

2. Experimental method

Torsion experiments were performed on single crystals artificially grown in the laboratory. The initial dislocation density of the sample was estimated to be less than 10^8 m^{-2} [16]. Samples were cylindrical, and grips consisted in refrozen water at the interface with the torsion device. Three different samples were tested (see characteristics in Table 1). A constant torsion torque was applied to each sample in order to obtain a shear stress of $0.2 \pm 0.05 \text{ MPa}$ on the surface. The temperature was maintained at $-15 \pm 1 \text{ }^\circ\text{C}$. The orientation of

the samples was chosen to align the torsion axis as close as possible to the c -axis. Basal planes were then parallel to the permanent shear plane. The shear strain varies with radius R of the cylinder such that $\gamma = \kappa R$, where κ is the twist per unit length. Shear strains reached 7% for samples 1 and 2, and 4% for sample 3. Creep curves are given in Fig. 1 for sample 1. The shear strain rates reached at the end of each test were between 2×10^{-6} and $5 \times 10^{-6} \text{ s}^{-1}$ (Table 1). A line marked on the sample was used to check homogeneity of the deformation along the torsion axis. After testing, samples were maintained at $-18 \text{ }^\circ\text{C}$.

In order to observe lattice distortion created during the torsion test, hard X-ray diffraction experiments were performed on samples taken from the cylinders. These experiments were carried out at the Institut Laue Langevin (ILL) in Grenoble, using an industrial high-voltage X-ray tube (420 kV) and the original Laue hard X-ray technique that allows in situ observation of bulk samples more than 1 cm thick [17]. The energy range for the white divergent beam is between 100 and 400 keV, resulting in wave lengths between 0.03 and 0.12 Å. Bragg angles being low, the diffraction peaks are located close to the direct beam, thus enabling simultaneous observation of peaks from several crystallographic planes. An X-ray intensifier and a CCD camera were used for fast acquisition of diffraction patterns. The width of the diffraction peaks is directly related to lattice distortion [17]. Angular lattice distortion from 10 s up

Table 1
Conditions for the torsion tests

Sample	1	2	3
Diameter (mm)	20	30	40
Height (mm)	50	61	59
Maximum applied shear stress (MPa)	0.2	0.2	0.18
Maximum shear strain	0.07	0.07	0.04
Maximum shear strain rate ($\text{s}^{-1}) \times 10^6$	3.8	4.6	2.5

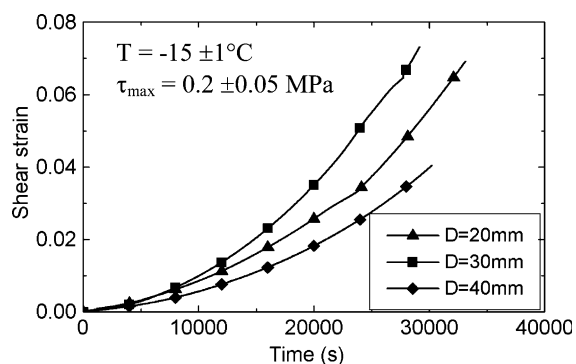


Fig. 1. Creep curves obtained during torsion tests on samples 1–3.

to a few degrees, depending on the sample-beam source distance, can be determined with this technique. The setup used for the present study has a measurement accuracy of better than 1 min of arc, taking into account the other broadening effects (size of the X-ray tube filament and sample thickness). Lattice distortion can be due to randomly located dislocations, inducing mosaicity which is associated with a homogeneous enlargement of the diffracted lines. Dislocations can also be arranged continuously within the crystal, creating lattice distortions (such as bending) that are represented by a continuous inclination of the lines. Both diffraction-line characteristics (mosaicity and inclination) can be analysed in terms of dislocation density. However, in the case of mosaicity, no simple direct relationship can be established due to the random spatial distribution of dislocations [18].

In each deformed sample, one “X-ray” sample was analysed. Characteristics are given in Table 2. The *c*-axis was vertical and perpendicular to the beam direction. The diffraction pattern of a non-deformed single crystal is given in Fig. 2a. Little continuous lattice distortion ($<0.3^\circ$) was found on the basal diffraction line. The mosaicity on both (0002) and (10 $\bar{1}$ 0) lines was virtually equivalent to the accuracy limit of the experimental configuration ($\sim 1'$).

3. Results

Fig. 2b shows the diffraction pattern obtained for sample XR2. Distortion of the lattice as seen on the (10 $\bar{1}$ 0) diffraction line was too large to be

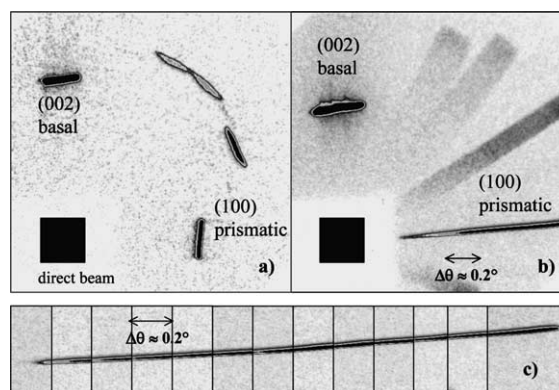


Fig. 2. Diffraction pattern obtained for sample XR2. (a) Diffraction pattern before deformation. The basal diffraction line is initially slightly distorted. (b) Global diffraction pattern after deformation. Only one part of the distortion of the (100) diffraction line is shown. (c) Reconstruction of the whole distortion of the (100) diffraction line by rotating the sample around the vertical axis.

observed in a single pattern. Reconstruction of the global (10 $\bar{1}$ 0) diffraction line was made possible by the rotation of the sample around the vertical axis (see Fig. 2c). Results concerning lattice distortion $\Delta\theta$ observed on prismatic (10 $\bar{1}$ 0) and basal (0002) diffraction lines are given in Table 2. A close estimate of the corresponding density of geometrically necessary dislocations is calculated as:

$$\rho_{\text{geom}} = \frac{\Delta\theta}{bD_c} \quad (1)$$

where *b* is the Burgers vector and *D_c* the size of the sample illuminated (height and length of the

Table 2
Sample characteristics for X-ray diffraction

X-ray sample	XR1	XR2	XR3
From sample no.	1	2	3
<i>L</i> × <i>h</i> × <i>e</i> (mm ³)	12 × 11 × 3	12 × 16 × 4	15 × 17 × 3
$\Delta\theta$ prismatic (°)	5.1	2.6	1.7
$\Delta\theta$ basal (°)	0.28	0.1	0.12
ρ_{geom} (m ⁻²) prismatic	17.4×10^9	8.4×10^9	3.9×10^9
ρ (m ⁻²) torsion strain	15.0×10^9	10.0×10^9	4.4×10^9

Distortion measurements on diffraction lines (basal and prismatic). Dislocations deduced from X-ray diffraction, ρ_{geom} (Eq. (1)) and from the torsion strain, ρ (Eq. (2)).

sample for calculation on the prismatic and basal lines respectively), see Table 2.

For the three samples studied, the reconstruction of the prismatic distortion pattern required rotation around the vertical axis to observe the entire distortion. The small width of the prismatic diffraction lines shows very little mosaicity (Fig. 2), as already observed on natural ice samples [14]. The continuous inclination of the diffraction lines indicates that torsion strain is not associated with the formation of twist boundaries. Edge dislocations cannot explain torsion of prismatic planes around the *c*-axis, therefore the large continuous distortion is explained by basal screw dislocations spread uniformly over the basal plane and inducing a rotation of the prismatic planes around the *c*-axis. Considering the little mosaicity on prismatic diffraction lines, the density of geometrically necessary dislocations calculated from Eq. (1) corresponds to the total density of basal screw dislocations within the sample.

Assuming only basal dislocations, distortion on the basal diffraction lines should be due to basal edge dislocations homogeneously positioned along the basal plane creating a regular bending of the planes along the sample [14]. While rotating the X-ray samples, we noticed very little mosaicity on the basal diffraction lines. The continuous distortion of the (0002) diffraction lines is low and corresponds to a dislocation density as low as that of the sample before deformation (Fig. 2a). We neglected it when considering the density of geometrically necessary dislocations associated with the torsion deformation.

To sum up, it appears that most of dislocations in the three samples studied are geometrically necessary. The main dislocations are of the screw type and the density increases as the diameter of the cylinder decreases.

4. Discussion

As observed in semiconductors with diamond structures, a continuous increase in the creep rate is observed with no apparent strain hardening (Fig. 1). The multiplication of mobile dislocations during deformation is the reason for the shape of

the creep curves [19]. The plastic properties of ice single crystals determined by uniaxial tension and compression are similar to those found in this study [20,21]. Strain rates calculated here for a strain of about 5% are of the same order of magnitude as those determined for other loading conditions. Easy basal slip characterises the behaviour of ice [22].

Since no hardening was observed in these creep tests, the density of dislocations accumulated during deformation is assumed to be too low to initiate significant elastic interaction between dislocations. The geometrically necessary dislocation density producing (or accommodating) the torsion of the lattice around the *c*-axis was determined from the distortion $\Delta\theta$ measured on the prismatic diffraction line (Table 2). The calculated density of these geometrically necessary dislocations can be compared with that deduced from the shear strain $\Delta\gamma$ in torsion which is given by:

$$\rho = \frac{\Delta\gamma}{Rb} \quad (2)$$

where $\Delta\gamma/R$ represents the twist per unit length and R the cylinder radius. A comparison is provided in Table 2.

The difference between the two values can be explained by the small volume analysed by X-ray diffraction and the possibility of a non-homogeneous distribution of dislocations within the sample. A non-homogeneous deformation was clearly visible through the shape of the line marked on sample 2, after the test. It was not the case for samples 1 and 3. The close values show that the torsion strain is fully associated with geometrically necessary basal screw dislocations.

Assuming that the hardening is due only to the interaction between geometrically necessary dislocations, the long-range stress is in the order of $(\mu b/2\pi)\sqrt{\rho}$ [9]. For example, the hardening associated with a dislocation density of $1.5 \times 10^{10} \text{ m}^{-2}$, as found in sample XR1, would correspond to a long-range stress of about $2.5 \times 10^4 \text{ Pa}$. This stress is significantly lower than the maximum shear stress applied in the torsion tests, which is in accordance with the absence of hardening in the torsion tests. Such hardening is expected to affect the creep rate at high strains or low stresses. In

polar ice sheets, deviatoric stresses being generally much lower than 0.1 MPa and strain much higher than 1 [23], hardening associated with strain gradients could take place.

The density of dislocations calculated from a physical deformation model by Montagnat and Duval [24] is higher than $2 \times 10^{10} \text{ m}^{-2}$ for a large portion of the Antarctic and Greenland ice sheets. Assuming that most dislocations in ice crystals are geometrically necessary, as found in this study and in Montagnat [14], a grain-size effect induced by the mismatch of slip at grain boundaries may be present [1,10].

In conclusion, this work clearly shows the relationship between the density of geometrically necessary dislocations and strain gradients. The torsion strain in the single crystal appears to be totally accommodated by geometrically necessary dislocations of the screw type, and statistically stored dislocations are negligible.

The variation of the density of geometrically necessary dislocations with the diameter of samples can be considered as a first size effect. The size-dependence strength should be observed as soon as hardening induced by the interaction between dislocations becomes significant. Torsion tests performed on ice single crystals at low shear stresses and relatively high shear strain are in progress to check this.

Ice may be a good model to study the relationship between the size-dependence strength and geometrically necessary dislocations. The expected large length scale could make this analysis easier.

Acknowledgements

This work was supported by CNRS, Département des Sciences Pour l'Ingénieur (SPI) (Programme Matériaux). We are very grateful to P. Sassin and F. Dominé for providing samples. We

thank O. Brissaud for the design of the cooling device and the help during the experiments, as well as ILL staff and particularly C. Menthonnex and A. Elaazzouzi for technical and computing assistance. Helpful comments of J. Gil Sevillano were appreciated.

References

- [1] Fleck NA, Muller GM, Ashby MF, Hutchinson JW. *Acta Metall Mater* 1994;42:475.
- [2] Fleck NA, Hutchinson JW. *J Mech Phys Solids* 1997;41:1825.
- [3] Nix WD, Gao H. *J Mech Solids* 1998;113:1.
- [4] Acharya A, Bassani JL. *J Mech Solids* 2000;48:2000.
- [5] Smyshlyayev VP, Fleck NA. *J Mech Phys Solids* 1996;44:465.
- [6] Kamijo T, Adachihara H, Fukutomi H. *Acta Metall Mater* 1993;41:9757.
- [7] Panchanadeeswaran S, Doherty RD, Becker R. *Acta Mater* 1996;44:1233.
- [8] Sun S, Adams BL, King WE. *Phil Mag* 2000;80:9.
- [9] Friedel J. *Dislocations*. New York: Pergamon Press; 1964.
- [10] Ashby MF. *Phil Mag* 1970;13:399.
- [11] Fleck NA, Ashby MF, Hutchinson JW. *Scripta Mater* 2003;48:179.
- [12] Needleman A, Gil Sevillano J. *Scripta Mater* 2003;48:109.
- [13] Gao H, Huang Y. *Scripta Mater* 2003;48:113.
- [14] Montagnat M, Thèse de doctorat, Université Joseph Fourier 2001.
- [15] Hondoh T. *Physics of ice core records*. Sapporo, Japan: Hokkaido University; 2000. p. 3–24.
- [16] Montagnat M, Duval P, Bastie P, Hamelin B, Brissaud O, De Angelis M, Petit JR, Lipenkov V. *C R Acad* 2001;333:419.
- [17] Hamelin B, Bastie P. *J Phys IV France* 1998;8:3.
- [18] Borbély A, Driver H, Hungar T. *Acta Mater* 2000;48:2005.
- [19] Johnston J. *J Appl Phys* 1962;33:2716.
- [20] Higashi A, Koinuma S, Mae S. *Jpn J Appl Phys* 1964;3:610.
- [21] Jones SJ, Glen JW. *J Glaciol* 1969;8:463.
- [22] Duval P, Ashby MF, Anderman I. *J Phys Chem* 1983;87:4066.
- [23] Alley RB. *J Glaciol* 1992;38:245.
- [24] Montagnat M, Duval P. *Earth Planet Sci Lett* 2000;183:179.